Binary colloidal systems in two-dimensional circular cavities: Structure and dynamics†

K. Mangold,[a] J. Birk,[a] P. Leiderer[a] and C. Bechinger[b]

[a] *University of Konstanz, Physics Department, 78457 Konstanz, Germany. E-mail: konrad.mangold@uni-konstanz.de; Fax: +49 7531 88 3127; Tel: +49 7531 88 3856*
[b] *University of Stuttgart, 2. Physikalisches Institut, Pfaffenwaldring 57, 70550 Stuttgart, Germany. E-mail: c.bechinger@physik.uni-stuttgart.de; Fax: +49 711 685 5285; Tel: +49 711 685 5218*

We study the melting behavior of a binary system ($R = 4.5$ μm, $r = 2.8$ μm) of paramagnetic colloidal spheres in two-dimensional (2D) circular cavities. A repulsive interaction between the particles is caused by an external magnetic field B that induces magnetic dipole moments perpendicular to the sample plane. By means of video microscopy, we investigate the positions of the particles and their trajectories. For small interaction strengths, we observe a completely liquid phase where large and small particles diffuse across the entire system. With increasing B the larger particles become—due to their larger magnetic moment—localized and form a stable structure while the smaller particles behave still as a liquid. For even higher magnetic fields, the small particles also become increasingly localized and preferentially arrange as interstitial sites between the structures formed by the large particles. We present a systematic study of this rather complex multi-stage melting process which strongly depends on the particle numbers of large and small particles.

Introduction

The study of two-dimensional (2D) few body systems in lateral confinements has made considerable progress in the last few years. Typical examples for clusters in three-dimensional (3D) and 2D systems are ions in radio-frequency traps,[1] electrons on the surface of liquid He,[2,3] or electrons in a quantum dot structure.[4] In addition the structural and dynamical properties of few body systems are also attractive from the theoretical point of view. Several authors considered 2D systems with finite numbers of ions or electrons in lateral confinements using Monte Carlo (MC)[5–9] or molecular dynamics[10] simulations. For small numbers of particles, the system does not crystallize in a triangular lattice as known for infinite systems (Wigner crystal)[11–14] but the structure of finite clusters is dominated by the geometry of the confining boundary.[15] In circular cavities, *e.g.* the particles form a concentric shell structure.[8,9,16]

The melting scenario of few-particle systems in circular cavities was also investigated by experiments[17,18] where an unexpected re-entrant melting was found. It has been experimentally demonstrated that at low effective temperatures the particles are arranged in a shell-like structure with high radial and angular order. Upon increasing the temperature T_{eff}, first intershell rotation sets in where the orientational order between adjacent shells is lost. As the temperature is increased further, however, orientational order is restored again.

This scenario was also confirmed by Brownian dynamics (BD) simulations of Schweigert *et al.*[19] who demonstrated that the angular diffusion coefficient shows a non-monotonic behavior as a function of the effective temperature. Since the decrease of the angular motion at high T_{eff} is accompanied by an increase of radial particle excursions, this suggested that the observed "reentrance" behavior is due to radial particle fluctuations which lead to an enhanced effective coupling between adjacent shells and thus to a reduction of intershell rotation.

While most of the numerical and experimental studies regarding finite size systems were performed with monodisperse particles, only very little is known about the behaviour of bi- and polydisperse systems in lateral confinements. It can be expected that owing to additional size effects, the phase behaviour is even more complicated. In the following we present investigations of repulsive binary colloidal systems in circular cavities. For small interaction strengths, we observe a completely liquid phase where large and small particles diffuse across the entire system. With increasing B the larger particles become—due to their larger magnetic moment—localized and form a stable structure while the smaller particles behave still as a liquid. For even higher magnetic fields, the small particles also become increasingly localized and preferentially arrange as interstitial sites between the structures formed by the large particles.

Experimental setup

The experiments were performed with an aqueous suspension of mixtures of superparamagnetic spheres with diameters of 4.5 and 2.8 μm, respectively. Both species consist of porous polystyrene particles doped with small clusters of iron-oxide (DynaBeads). The particles are coated additionally with a thin epoxy layer to prevent the magnetic clusters from being washed out into the solution. The size and distance of the magnetite clusters is sufficiently small to consider each cluster as magnetically independent. Accordingly, in the absence of an external magnetic field B, the magnetic moments of the clusters are orientated randomly and the effective magnetic moment of the sphere vanishes. In the presence of an external magnetic field the magnetic dipoles are aligned parallel to B which leads to a macroscopic magnetic moment of the spheres.

† Presented at the 17th Conference of the European Colloid & Interface Science Society, Firenze, Italy, September 21–26, 2003.

The particle pair potential $V(r)$ is dominated by a magnetic dipole interaction which can be adjusted by the external magnetic field B due to the superparamagnetic properties of the spheres. B induces a magnetic dipole moment M_i in each sphere i. In a 2D system (as is the case in our experiments as described below) with perpendicular magnetic field this leads to a repulsive magnetic dipole pair potential $V_{i,j}^{\mathrm{mag}}(r) = \mu_0 M_i M_j / 4\pi r_{i,j}^3$, where $r_{i,j}$ is the particle distance.[15,20] The B-field dependence of the magnetic moment is well known to correspond to the Langevin function. For the magnetic fields as used in this work, however, the magnetic moment increases in a linear way with B.

The colloidal suspension was stabilized with SDS (sodium dodecyl sulfate), to prevent the particles from sticking together when the external magnetic field is turned off. Additionally we added antibiotics and thimerosal to avoid contamination of the suspension with organic impurities. This allowed us to obtain stable conditions over several weeks.

We determined the magnetic moments of the spheres by comparing the experimentally measured pair correlation functions of diluted monodisperse suspensions with appropriate data from numerical simulations. From this we obtained for the magnetic moment of a large particle $M_{\mathrm{big}} = (3.1 \pm 0.02) \times 10^{-11}$ A m^2 T^{-1} B^{-1} and for the small particles $\mathrm{M}_{\mathrm{small}} = (3.9 \pm 0.1) \times 10^{-12}$ A m^2 T^{-1} B^{-1}. The ratio of $M_{\mathrm{big}}/M_{\mathrm{small}}$ is in good agreement with assuming that the magnetic moment of the spheres scales in a linear way with the amount of the superparamagnetic material, *i.e.* the particle volume.

As shown in Fig. 1 the substrate for the 2D colloidal system was made of a silica plate covered with a 1 μm thick smooth film of PMMA (poly(methylmethacrylate)) which was deposited by spin-coating. This film is necessary to prevent the particles from sticking to the surface. Lateral confinements were realized by pressing a copper TEM (transmission electron microscope) grid into the heated PMMA film. After this procedure we obtained several tens of identical compartments with perpendicular walls of about 15 μm height and a circular shape with a diameter of 73 μm. For the details of the sample preparation we refer to the literature.[15]

When the sample cell was filled with colloidal suspension, the particles, owing to their density (1.5 g cm^{-3}), started to sediment towards the bottom plate where they formed a 2D system in each compartment.

The number density n_{b} of big and small n_{s} particles in the compartments varied statistically in a range between 20 and 50 depending on the particle concentration in the suspension. The whole cell was placed in the centre of a pair of Helmholtz coils to produce a magnetic field B perpendicular to the substrate.

The colloidal spheres were imaged with a home-built inverted video microscope. In time intervals which were on the order of several seconds a picture was taken and a particle recognition algorithm was used to determine particle coordinates and particle areas for each frame of the sequence. Since small and large particles clearly differ in area, we could easily distinguish between the two species.

To describe the state of a monodisperse system, the dimensionless ratio of the magnetic energy and the thermal energy is used. This quantity is known as plasma parameter $\Gamma = \langle V^{\mathrm{mag}} \rangle / N k_{\mathrm{B}} T$, where the brackets correspond to the sum over all pairs i,j, N corresponds to the number of particles and $k_{\mathrm{B}}T$ to the thermal energy. In our case, however, we have to consider two different magnetic moments and therefore three possible interaction energies. Therefore, we calculated Γ for each frame by summing up the pair interaction potentials for each particle configuration. We used the measured distances and the appropriate magnetic moment of the particles to obtain the total interaction potential for each frame.

$$V^{\mathrm{mag}} = \mu_0/4\pi \Big(\sum M_i^{\mathrm{big}} M_j^{\mathrm{big}} / r_{i,j}^3 + \sum M_i^{\mathrm{small}} M_j^{\mathrm{small}} / r_{i,j}^3 + \sum M_i^{\mathrm{big}} M_j^{\mathrm{small}} / r_{i,j}^3 \Big)$$

When averaging these values over all frames we obtained an effective Γ that characterizes the entire sequence and which is characteristic for the experimental conditions. Since B plays the role of an inverse effective temperature we varied B in our experiments and kept the temperature constant at $T = 195$ K.

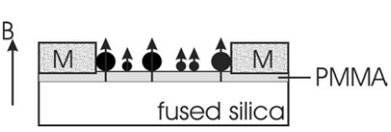

Fig. 1 Schematic side view of a section of the experimental cell. A TEM mesh (M) serves as lateral confinements for the particles.

Results

A typical snapshot of a system with 38 large and 10 small particles is shown in Fig. 2a. Here, the diameter of the whole system is 73 μm. The larger particles form a shell structure with one particle in the innermost shell (slightly off-centre the circular compartment), an inner shell with 5 particles, an intermediate shell with 11 particles and an outer shell with 21 particles, respectively. We will refer to this as (1,5,11,21)-configuration. In the absence of additional smaller particles, the ground state of such a system corresponds to a (1,6,11,20) configuration, as shown by numerical simulations.[21] Obviously, the presence of the 10 smaller particles leads only to a slight modification of the ground state compared to the monodisperse system. To compare our experimental results with numerical results we also performed MC simulations which are based on the method of simulated annealing. With the help of the simulations we found that the ground state of a system with fixed numbers of small and large particles is nearly degenerated, with potential energy differences close to the ground state of only one-tenth of a percent.

Fig. 2b shows the ground state of a simulation of 38 large and 10 small particles. While our simulation essentially reproduced the observed configuration of the large particles, minor differences in the positions of the small particles are observed. This, however, is attributed to the above mentioned small energy differences around the ground state and the rather long time-scales the system requires to find its true ground state.

In order to study experimentally the melting behaviour of finite binary systems, we systematically varied the effective particle interaction via the external magnetic field. In an exemplary manner we show in Fig. 3a–d particle density plots for a melting process of a system with 32 large (black) and 35 small (grey) particles. The system resides in a solid state at $\Gamma = 12.8$ (Fig. 3a) where the large and the small particles are rather localized. Due to the larger magnetic moment, the larger particles occupy the edge of the confinement. With decreasing particle

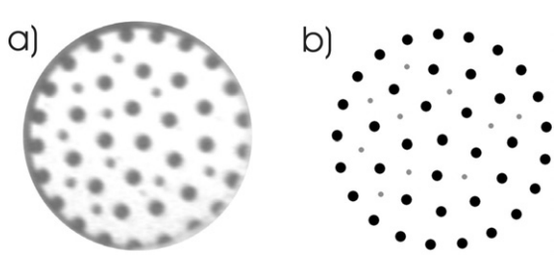

Fig. 2 Ground state of a system with 38 large and 10 small particles. (a): real space image (diameter of circular cavity: 73 μm), (b): MC simulation.

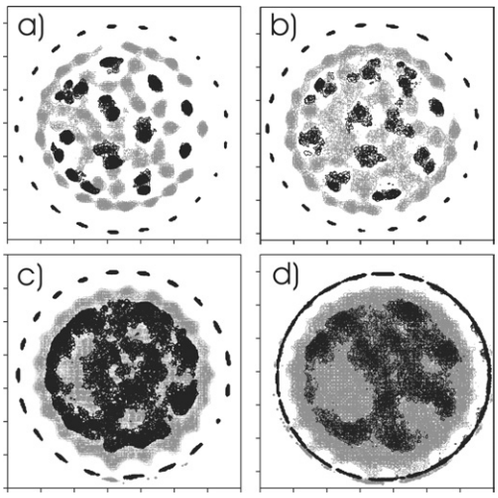

Fig. 3 Particle density plots for 32 large (black) and 35 small (grey) particles. (a) For $\Gamma = 12.8$ the large and small particles are rather well located, (b) for $\Gamma = 8.7$ the larger particle are rather fixed but the small ones can still diffuse in the matrix of large particles, at (c) for $\Gamma = 4.3$ the larger particles begin to move and form a shell structure, and (d) for $\Gamma = 1.0$ no order is obvious. The axis ticks correspond to 10 μm.

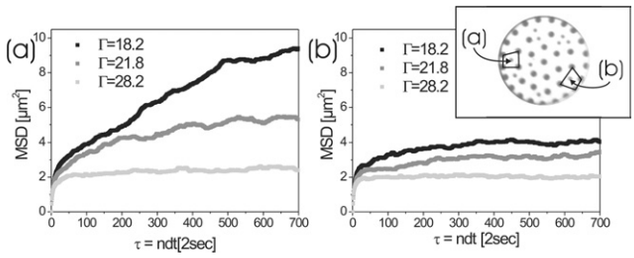

Fig. 4 Mean square displacements (MSD) for different Γ values of two small particles in unequal environments. The configuration of the large particles around a small particle affects the dynamic behaviour of the small particle significantly. For $\Gamma = 28.2$ the MSD of the two small particles (a) and (b) is saturated, this is a signature of the solid state. For $\Gamma = 18.2$ the MSD of (b) is still saturated, but the MSD of (a) still increases.

interaction, *i.e.* $\Gamma = 8.7$ (Fig. 3b) the smaller particles become mobile while the larger particles are still localized. For even smaller particle interaction ($\Gamma = 4.3$) the larger particles start also to diffuse over substantial distances, but still a shell structure of the larger particles is noticeable (Fig. 3c). In comparison to Fig. 3b the configuration of the larger particles changed from a (3,8,21) to a (3,9,20) system. At very small particle interactions ($\Gamma = 1.0$) the most conspicuous structure is the ring of larger particles at the edge of the confinement and a small zone nearby where the small particles cannot intrude (Fig. 3d). In comparison with a monodisperse system of 32 particles[22] where the ground state corresponds to a (4,10,18) configuration for the binary system we observe a (3,8,21) configuration. This difference is obviously caused by the presence of the smaller particles which can be considered as an effective background to the larger particles which modifies the effective potential of the large particles. It is well known from other (not dipolar) pair potentials that the ground state configurations sensitively depend on the effective pair interactions.[8,9,19,23,24]

In addition to the configuration shown in Fig. 3 we also investigated systems with other number densities of large and small particles. Although the melting scenario depends strongly on the particle densities and the configuration of the system, in general the two-step melting occurs as described for the system in Fig. 3.

Another typical feature of a binary system in the solid phase is the circular arrangement of larger particles at the edge of the confinement. This is due to the strong particle repulsion and leads to a pressure onto the circular wall. The difference of the magnetic moments of the two particle types is so huge, that a small particle in the outer ring leads to a very unstable configuration. For Γ-values close to the melting transition the large particles are able to escape from this outer ring and the system is likely to undergo a change in the configuration. In general the tendency for changing the configuration is much higher than in a monodisperse system.

During our experiments with different particle densities we found indications toward a re-entrant phase transition similar to that observed in monodisperse systems, but up to now clear evidence is absent. More detailed numerical studies and experiments will be required.

Since the data acquisition speed was large compared to the typical particle velocities, in addition to the static properties we also obtained dynamical information. In Fig. 4 we show as an example the mean square displacements (MSD) of two small particles which are identified by the inset of Fig. 4b. Within a time interval τ a single particle undergoes the quadratic displacement $\Delta r^2(\tau) = [\vec{r}(t+\tau) - \vec{r}(t)]^2$. To obtain the mean square displacement (MSD) of a particle, we average Δr^2 over all possible starting times t. The smallest time resolution in our experiments is given by the time dt between two successive frames, therefore τ has to be a multiple of dt. Since dt was chosen in our experiments to be d$t = 2$ s, no information about the particle movement on shorter time scales was obtained.

Fig. 4 shows the MSD of two small particles with slight different local environments (*i.e.* configuration of large particles) in the same system (see inset of Fig. 4b). When the interaction potential between the particles is high ($\Gamma = 28.2$) the MSD of the two particles show a similar behaviour, *i.e.* a sharp increase at small times which is followed by a saturation above $\tau = 40$ s. This saturation is characteristic for systems where the accessible space of a particle is limited. In the situation discussed here, this limitation is obviously caused by the big particles surrounding the small particles (solid lines in the inset of Fig. 4) which form an effective cage for the small particles. When the particle interaction is lowered ($\Gamma = 21.8$) the effective size of the cage is increased and the small particles can explore a larger area. This explains why the plateau of the MSD in Fig. 4a,b is shifted to somewhat larger values. For even smaller particle interaction ($\Gamma = 18.2$) the difference between the two particles (a) and (b) is obvious. While particle (b) is still localized inside a cage of the surrounding particles, particle (a) escapes the local cage and performs a diffusion process, as seen by the linear increase of the MSD. A qualitatively similar behaviour is also found in glass-like systems where the dynamics is also governed by escape and trapping of particles in cages.

In summary, we have studied the melting of binary colloidal 2D systems in a circular cavity. The experimentally observed ground states were compared to additionally performed MC simulations. For these systems a rather complex multi-stage melting process is found. The structure of the colloids is found to be influenced by the circular hard-wall potential, therefore the big particles arrange in a shell-like structure which depends on the number of particles and on the ratio of big and small colloids. The melting process takes place in several steps where first the small particles and only then the large ones become delocalized. In addition we also found that the dynamics of the system shows typical glass like features.

Acknowledgements

This work was supported by the Deutsche Forschungsgemeinschaft (SFB 513).

References

1 G. Birkl, S. Kassner and H. Walther, *Europhys. News*, 1992, **23**, 143.
2 See, *e.g.*, *2D Electron Systems on He and Other Cryogenic Substrates*, ed. E. Andrei, Kluwer Academic Publishers, Dordrecht, The Netherlands, 1998.
3 P. Leiderer, *J. Low Temp. Phys.*, 1992, **87**, 247.
4 M. A. Reed and W. P. Kirk, *Nanostructure Physics and Fabrication*, Academic Press, Boston, 1989.
5 Y. E. Lozovik and V. A. Mandelshtam, *Phys. Lett. A*, 1990, **145**, 269.
6 Y. E. Lozovik and V. A. Mandelshtam, *Phys. Lett. A*, 1992, **165**, 469.
7 F. M. Peeters, V. A. Schweigert and V. M. Bedanow, *Physica B*, 1995, **212**, 237.
8 V. M. Bedanow and F. M. Peeters, *Phys. Rev. B*, 1994, **49**, 2667.
9 V. A. Schweigert and F. M. Peeters, *Phys. Rev. B*, 1995, **51**, 7700.
10 J. A. Drocco, C. J. Olson Reichhardt, C. Reichhardt and B. Janko, *Phys. Rev. E*, 2003, **68**, 6040(R).
11 J. M. Kosterlitz and D. J. Thouless, *J. Phys. C*, 1973, **6**, 1181.
12 D. R. Nelson and B. I. Halperin, *Phys. Rev. B*, 1979, **19**, 2457.
13 A. H. Marcus and S. A. Rice, *Phys. Rev. E*, 1997, **55**, 637.
14 K. J. Strandburg, *Rev. Mod. Phys.*, 1988, **60**, 161.
15 R. Bubeck, S. Neser, C. Bechinger and P. Leiderer, *Prog. Colloid Polym. Sci.*, 1998, **110**, 41.
16 Y. E. Lozovik and E. A. Rakoch, *Phys. Lett. A*, 1997, **235**, 55.
17 R. Bubeck, C. Bechinger, S. Neser and P. Leiderer, *Phys. Rev. Lett.*, 1998, **82**, 3364.
18 R. Bubeck, P. Leiderer and C. Bechinger, *Prog. Colloid Polym. Sci.*, 2001, **118**, 73.
19 I. V. Schweigert, V. A. Schweigert and F. M. Peeters, *Phys. Rev. Lett.*, 2000, **84**, 4381.
20 K. Zahn, J. M. Mendez and G. Maret, *Phys. Rev. Lett.*, 1997, **79**, 175.
21 P. Henseler, Diploma Thesis, University of Konstanz, 2002.
22 R. Bubeck, PhD Thesis, University of Konstanz, 2002.
23 Y. E. Lozovik and E. A. Rakoch, *JETP*, 1999, **89**, 1089.
24 A. I. Belousov and Y. E. Lozovik, *Eur. Phys. J. D*, 2000, **8**, 241.